IEEE Photonics Journal
An IEEE Photonics Society Publication

Open Access

Damping Microvibration Measurement Using Laser Diode Self-Mixing Interference

Volume 6, Number 3, June 2014

Minliang Chen
Yongbing Zhang
Chenxi Chen
Lu Wang
Wencai Huang

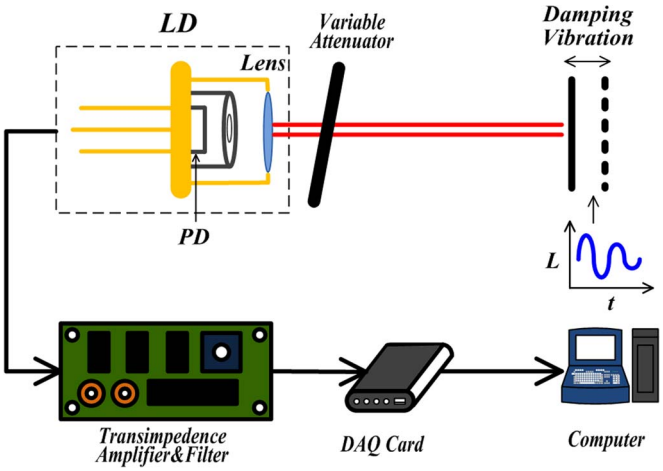

DOI: 10.1109/JPHOT.2014.2323314
1943-0655

Damping Microvibration Measurement Using Laser Diode Self-Mixing Interference

Minliang Chen, Yongbing Zhang, Chenxi Chen, Lu Wang, and Wencai Huang

Department of Electronic Engineering, Xiamen University, Xiamen 361005, China

DOI: 10.1109/JPHOT.2014.2323314

Manuscript received March 23, 2014; revised April 24, 2014; accepted May 2, 2014. Date of publication May 13, 2014; date of current version May 23, 2014. This work was supported by the National Natural Science Foundation of China under Grant 61108019. Corresponding author: W. Huang (e-mail: huangwc@xmu.edu.cn).

Abstract: Based on the study of laser diode self-mixing interference effects, a simple damping microvibration measuring method that can accurately obtain the damping factor is presented. The damping factor is solved by recording the period and counting the fringe number of the self-mixing signal. The damping factor of 0.0483 s^{-1} with a standard deviation of 0.0013 and the coefficient of variation of 2.69% was experimentally achieved. Theoretical simulation of the feedback strength on the measuring accuracy shows that the measuring method of the damping factor has high accuracy in the case of weak feedback.

Index Terms: Self-mixing interference, damping factor, microvibration.

1. Introduction

Vibration phenomenon plays an important role in nature and engineering. Study of the vibration is helpful to discover and solve problem in the processing of industrial engineering product. However, the damping is a nonnegligible element in the mechanical world, and it is a fundamental parameter of structural vibration analysis, which can reflect the properties of material. Therefore, not only in engineering application but also in material analysis, it is necessary to determine the actual damping factor through various methods. Wojtowicki *et al.* [1] applied a free–free beam (composite cantilever Oberst beam) to the measurement of the damping properties of material. Ouis [2] presented a measurement of damping in solid materials by means of a room acoustical technique. Cai *et al.* [3] reported a technique that can measure the damping properties of material based on an electromagnetic shaker. However, test systems of these methods are very complex structures. Meanwhile, in traditional measurements of vibrations, devices are limited by having association with the target object, such as accelerometers or strength gauges. The reason is that these devices often changes the displacements and frequency characteristics of the test object and are inconveniently used in a hostile environment. In past several decades, along with the development of optical techniques in measuring field, the laser techniques, with the characters of high spatial resolution, rapid responses and antielectromagnetic interference, has attracted considerable attention. Particularly in some high-temperature or high-pressure conditions, noncontact optical measurement has its incomparable advantage.

In this paper, we present a simple damping microvibration measuring method using a laser diode (LD) self-mixing interferometry (SMI) [4]. In past several decades, the applications of the SMI have been popularized in many fields, including absolute distance [5], [6], velocity [7] or flow speed [8], [9],

vibration [10]–[12], and some laser parameters [13]. Compared with other traditional interference like the Michelson interference, the advantages of SMI are its low cost and compactness, merely needing a laser and a photodiode (PD). The optic path is very simple and self-aligning that does not require a reference path. In next sections, through the theoretical simulation and experiment, we will give the details about this method and prove its feasibility that can measure the damping factor with relatively high accuracy.

2. Method for Damping Vibration Measurement

2.1. Theory of the Self-Mixing Interference

As we all know, when the light reflected or back-scattered by the external target reenters the laser cavity, the frequency and power of emitting light will be modulated. Although the frequency modulation is difficult to detect because of the quite high optical frequency, the change of optical power can be easily available by observing the current detected by the PD, which is packaged in the LD. The self-mixing interference effect has been studied deeply and described by [14], [15], and based on an analytical steady-state solution, the emitted power P is often expressed as

$$P(\phi) = P_0[1 + mF(\phi)] \tag{1}$$

The laser phase is subject to the feedback given by the phase equation

$$\phi = \phi_0 - C\sin[\phi + \arctan(\alpha)] \tag{2}$$

In the equation (1) and (2), P_0 is the laser power without optical feedback and m is the modulation index. ϕ_0 is the optical phase of the external path in the absence of feedback, given by $\phi_0 = 2kL = 4\pi L/\lambda$ with k being the wave vector, λ being the wavelength and L being the variation of distance from the LD to the target. ϕ is the optical phase with feedback. $F(\phi)$ is a periodic function whose shape depends on the feedback strength parameter C [16], which, in turn, depends on laser parameters, mismatch coefficient, target distance, and laser cavity length. When the system stays in weak feedback regime, $F(\phi)$ is a cosine function, like expected in a normal interferometer. In our design, in order to reduce the error caused by phase shift that is analyzed in the discussion section, we would only stay in the very weak self-mixing regime $(C \gg 1)$ in the experiment.

2.2. Simulation and Signal Processing

According to the theory of damping vibration [17], we can get the equation of motion of the system. It can be written as

$$S\ddot{L}(t) + D\dot{L}(t) + ML(t) = f(t) \tag{3}$$

where $f(t)$ is the stimulating force, $L(t)$ is the displacement of vibration, S, D and M are stiffness, damping and inertia operators, respectively. They are homogeneous differential operators with order depending on the characteristics of the vibration. In a single degree-of-freedom (SDOF) system, when the stimulating force $f(t)$ is removed, the equation of motion of the system can be written as

$$\ddot{L}(t) + 2\beta\dot{L}(t) + \omega_0^2 L(t) = 0 \tag{4}$$

where β is the damping factor, ω_0 is the natural angular frequency, t is the time variable. In most instances $0 < \beta < \omega_0$, the system forms a natural damping vibration and can be solved as

$$L(t) = A_0\cos(\omega t + \varphi)e^{-\beta t} \tag{5}$$

$$\omega = \sqrt{\omega_0^2 - \beta^2\omega_0^2} \tag{6}$$

where A_0 is the initial amplitude, ω is the angular frequency with damping, and φ is the initial phase.

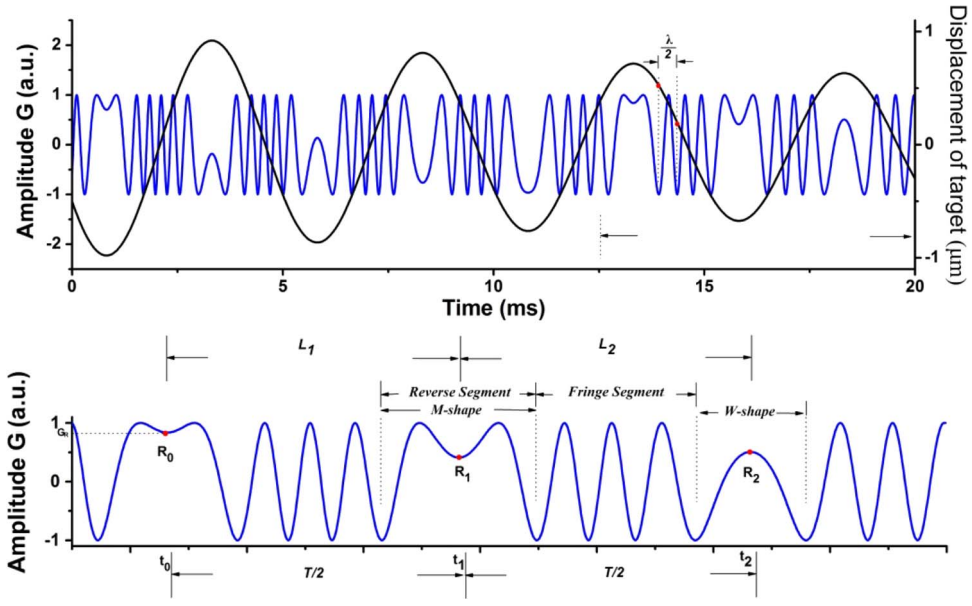

Fig. 1. (a) The displacement of target and the artificial SMS. (b) The region zoom in.

In our design, assuming that the displacement of target $(L(t))$ matches with equation (5). In the simulation, we set $A_0 = 1$ μm, $\omega = 400\pi$ rad/s, $\beta = 25$ s^{-1}, $\lambda = 650$ nm and use equation (1), (2) to generate a set of artificial self-mixing signal (SMS) samples (Fig. 1(a)). The black curve is the displacement of damping vibration and the blue curve is the corresponding simulated SMS. In the same period, SMS can be seen that the number of the fringes decreases over time. Each fringe corresponds to $\lambda/2$ change of displacement or 2π phase change of SMS.

Assuming that we obtain the actual measured signals like Fig. 1(b), the region we randomly zoom in Fig. 1(a). Now we will give the details for how to calculate the damping factor. There are some characteristic points marked by R $(\mathrm{R}_0, \mathrm{R}_1, \mathrm{R}_2 \cdots)$ in SMS. These points are called reverse points which indicate the position where the target changes its movement direction. The corresponding time points are marked by t $(\mathrm{t}_0, \mathrm{t}_1, \mathrm{t}_2 \cdots)$. According to the period of vibrations, the time interval between two arbitrary adjacent reverse points is the semiperiod (T/2). Therefore, the computed frequency can be expressed as

$$\hat{f} = \frac{1}{\hat{T}} = \frac{1}{2(t_1 - t_0)} \tag{7}$$

Of course, by taking Fourier transform of SMS, the frequency can be also obtained easily in frequency domain. After locating these reverse points, the corresponding estimated displacement of target $L'(t)$ in Fig. 1(b) is set as

$$L'(t) = A_0' \cos\left[2\pi \hat{f}(t - t_0)\right] e^{-\beta t} \tag{8}$$

Calculating the displacement (L_1, L_2) between every two points where the target changes its movement direction. Then we have

$$\begin{aligned} L(t_0) - L(t_1) &= A_0' - A_0' \cdot \cos\left(2\pi \hat{f} \frac{T}{2}\right) \cdot e^{-\beta \frac{T}{2}} = L_1 \\ L(t_2) - L(t_1) &= A_0' \cdot \cos(2\pi \hat{f}\, T) \cdot e^{-\beta T} - A_0' \cdot \cos\left(2\pi \hat{f} \frac{T}{2}\right) \cdot e^{-\beta \frac{T}{2}} = L_2 \end{aligned} \tag{9}$$

The accurate damping factor measuring method mainly depends on locating accuracy for those characteristic points as mentioned above and the displacement in one period or semiperiod in SMS.

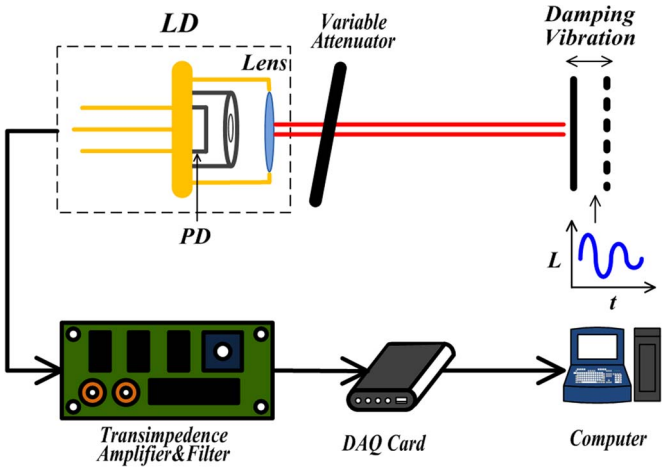

Fig. 2. Experimental setup to measure damping microvibration in SMI.

As is mentioned, in typical SMI system, each fringe corresponds to $\lambda/2$ change of displacement or 2π phase change of SMS. When N fringes appear for each semiperiod of the signal (fringe segment), the displacement is usually calculated as $L = N\lambda/2$ with the error $\lambda/2$. In actual SMS, the W-shaped or M-shaped waveform is often observed when the real displacement is bigger than $N\lambda/2$ and smaller than $(N+1)\lambda/2$. These waveforms are also caused by the different initial phase. Therefore, the displacement between two reverse points should be amended as

$$L = (N + N')\lambda/2 \tag{10}$$

N is the number of entire fringes and N' is the number of incomplete fringes. Hence, combining with equation (9), (10), we can obtain the simplified equation at the moment t_0

$$\beta\frac{T}{2} = In\frac{L_1}{L_2} = In\frac{N_{t_0} + N'_{t_0}}{N_{t_0+T/2} + N'_{t_0+T/2}} \tag{11}$$

As mentioned above, the actual incomplete fringes will vary to the M-shape or W-shape depending on the initial phase and the measured amplitude. When $C \ll 1$, considering the range of anticosine is from 0 to π and a fringe is equal to 2π phase shift, we can calculate the ratio of incomplete fringes to a full fringe (W-shaped is less than half fringe: $\pi - \arccos(G_R)$ or M-shaped is more than half fringe: $\pi + \arccos(G_R)$), hence, the parts of the number of incomplete fringes in reverse segment are approximatively given by

$$N_W = \frac{\pi - \arccos(G_R)}{2\pi}, \quad N_M = \frac{\pi + \arccos(G_R)}{2\pi} \tag{12}$$

where G_R is the normalized value of reverse point R marked as in Fig. 1(b). According to equation (11) and (12) the damping factor β can be solved though the parameter T and N which can be obtained from the SMS by signal processing. For the verification in the simulation (Fig. 1), the calculated average $\beta = 25.02$ is very close to the initial set.

3. Experiment and Results

The experimental setup is shown in Fig. 2. An LD (LD FU650AD5_C9N) is used as the light source, emitting up to 5 mW at 650 nm on a single longitudinal mode, fed by a constant current supply. The damping vibration source is placed at a distance of 20 cm from the laser. Variable attenuator is set to keep the weak feedback. A power-monitor PD packaged in the LD detects the changes of laser power and transforms light power into current, which will be amplified by a transimpedance amplifier and acquired by a computer via a DAQ card (ISDS205A).

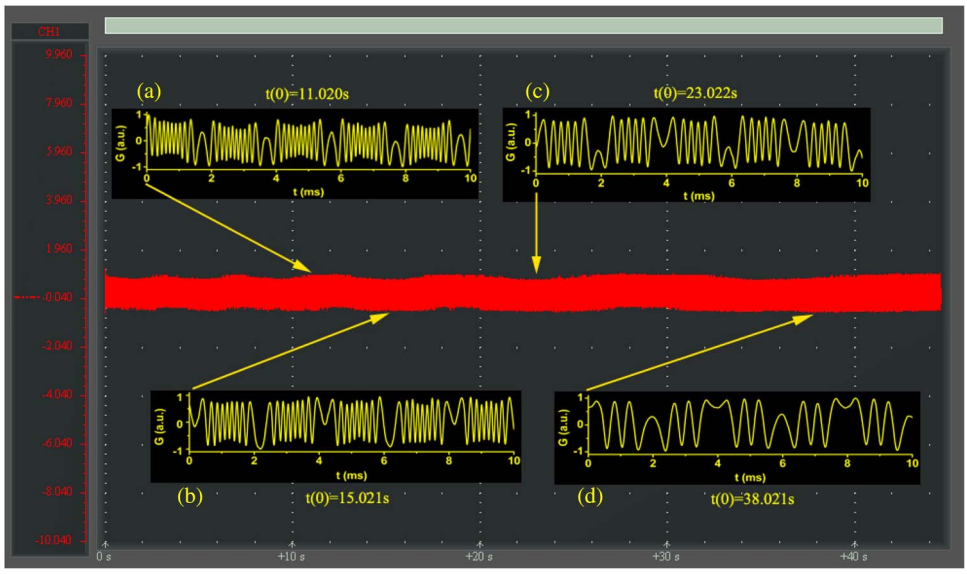

Fig. 3. Experimental results of the whole SMS and the typical signals (a)–(d) at different moments.

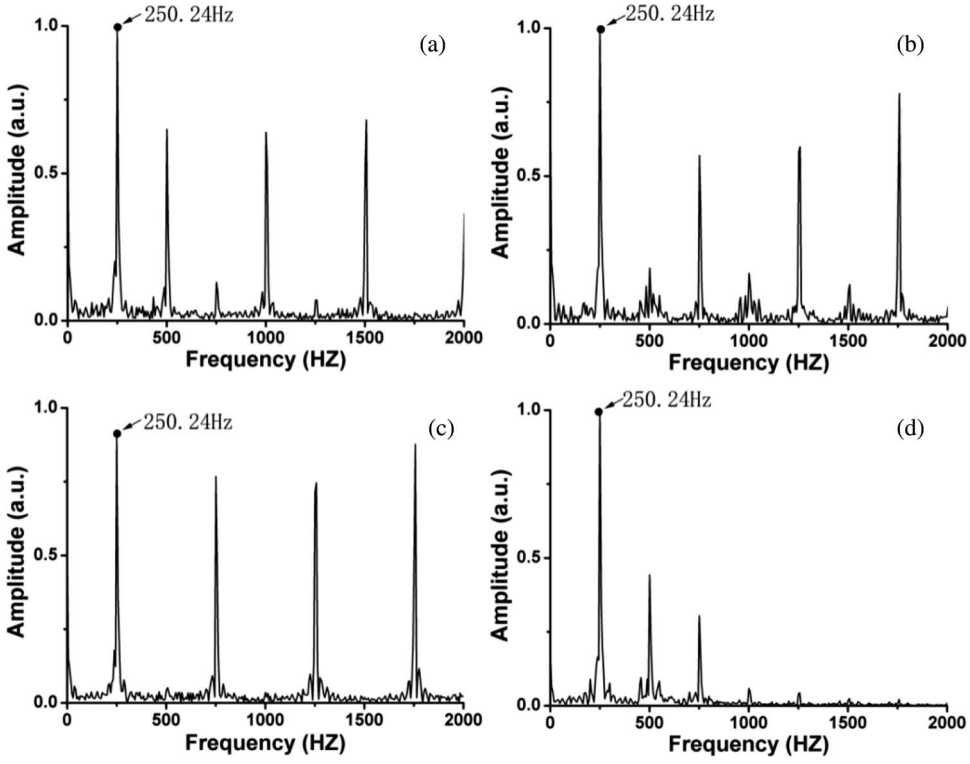

Fig. 4. Frequency spectra of SMSs shown in Fig. 3(a)–(d).

In the experiment, when the target object started damping vibration freely, the SMS of the whole process was recorded by the DAQ card, shown in Fig. 3. At different moments in a damping vibration, Graph (a)–(d) in Fig. 3 were the typical signals (started time corresponding points at 11.020 s, 15.021 s, 23.022 s, 38.021 s, respectively) that obviously showed the amplitude of the target were decreasing (the rough number of fringe from 10, 8, 6 to 3) over time due to the existence of the damping property. The corresponding frequency spectra are shown in Fig. 4. It can be seen

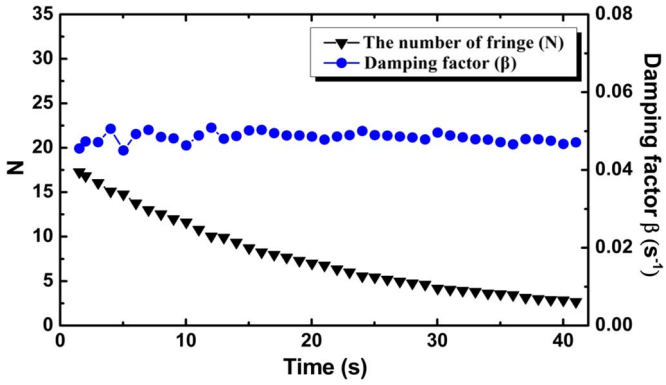

Fig. 5. The calculated results of damping factor at different time points.

that the basic peak of these four images all appeared at 250.24 Hz which indicates that the frequency of damping vibration is constant.

In the experiments, the amplitude of vibration attenuated slowly on account of the small damping factor. Therefore, in an image of SMS, it was hard to distinguish the change of the number of fringe between two adjacent periods. From the above theoretical analysis, damping factor depends on the ratio of the number of fringe between two time points, (12) could be fixed by

$$\beta\tilde{T} = In\left(\frac{N_{t_0}}{N_{t_0+\tilde{T}}}\right) \tag{13}$$

where $\tilde{T}$ is the enlarged interval between two images of SMS. N is the total number of fringe including incomplete fringes. Therefore, a SMS during 40 s was recorded for calculating the damping factor at different moments. Fig. 5 illustrates the number of fringe and the calculated damping factor value by sampling the SMS every second. Obviously, the number of the fringes decreased with the time increasing. The damping factor was 0.0483 s^{-1} with a small fluctuation. Its standard deviation was 0.0013 and the coefficient of variation was 2.69%.

4. Discussion

In Section 2.2, we set the feedback strength C very small. In fact, the feedback strength will affect the G_R and then cause the error of damping factor. As is well known, feedback strength is a significant parameter in laser self-mixing interference, which discriminates the different feedback regimes and changes the shape of SMS. According to equation (2), assuming the vibration of target L is sinusoidal for example, Fig. 6 presents simulation results for the two phases (ϕ and ϕ_0) at different feedback strength C. As can be seen from Fig. 6, larger C will lead to larger phase shift between ϕ and ϕ_0. The phase ϕ could be regarded as ϕ_0 merely when C is very small. Therefore, we should set the feedback strength C far less than 1 in order to decrease the error. To gain insight into the influence of C, we generated groups of SMS under different C and β. It is no doubt that larger β leads to the faster attenuation time of vibration. We set appropriate time interval to calculate the damping factor in different group of SMS by the method mentioned above. The results including average damping factor (Avg.), standard deviation (SD) and coefficient of variation (C.V) are shown in Table 1. The definition of C.V is

$$C.V = \frac{Avg.}{SD} \times 100\% \tag{14}$$

which can compare the dispersion degree for different average value. When C is small, the calculated average damping is very close to the true values no matter the β is small or large. Meanwhile, the small standard deviation and coefficient of variation demonstrate the results have a slight fluctuations in the case of $C < 0.1$. It can be seen that our experimental result is closed to the case

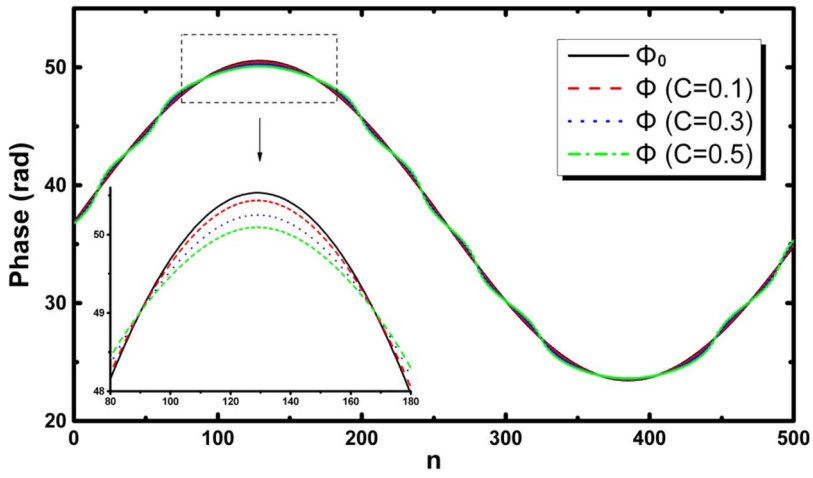

Fig. 6. The phase without feedback and the phase with feedback under different C.

TABLE 1

Influence of C on the calculation of β

C	True β=25			True β=1			True β=0.05		
	Avg.	SD	C.V	Avg.	SD	C.V	Avg.	SD	C.V
0.01	24.9801	0.1275	0.51	1.0000	0.0049	0.49	0.0500	0.00025	0.50
0.1	24.7920	1.1898	4.80	0.9997	0.0464	4.64	0.0495	0.0023	4.71
0.2	24.5656	2.4165	9.84	0.9994	0.0964	9.64	0.0490	0.0046	9.40
0.3	24.3229	3.5113	14.44	0.9992	0.1421	14.23	0.0484	0.0069	14.24

of C = 0.1 and $\beta = 0.05$ in simulated analysis of error due to the diffuse reflection of the target in experiment. So the system stayed in weak feedback regime readily. If the target has high reflectivity, we can fine-tune the variable attenuator or change the parameter of self-mixing interference system to guarantee the weak feedback for obtaining higher accuracy.

5. Conclusion

A simple method that can measure damping microvibration and calculate damping factor in laser SMI has been proposed. By fringe-counting accurately, the experimental result with small coefficient of variation was obtained; meanwhile, the error caused by feedback strength C is also discussed. This SMI approach presents potential application prospects in precise vibration measurement and material property analysis.

References

[1] J. L. Wojtowicki, L. Jaouen, and R. Panneton, "New approach for the measurement of damping properties of materials using the Oberst beam," *Rev. Sci. Instrum.*, vol. 75, no. 8, pp. 2569–2574, 2004.
[2] D. Ouis, "Measurement of damping in solid materials by means of a room acoustical technique," in *Proc. 9th Int. Symp. Nondestruct. Characterization Mater.*, 1999, pp. 587–592, American Institute of Physics.
[3] C. Cai and Q. Sun, "Measurement of damping properties of damping material," in *Proc. 6th Int. Symp. Precis. Eng. Meas. Instrum.*, 2010, pp. 75440S-1–75440S-7, International Society for Optics and Photonics.
[4] S. Donati, "Developing self-mixing interferometry for instrumentation and measurements," *Laser Photon. Rev.*, vol. 6, no. 3, pp. 393–417, May 2012.
[5] F. Gouaux, N. Servagent, and T. Bosch, "Absolute distance measurement with an optical feedback interferometer," *Appl. Opt.*, vol. 37, no. 28, pp. 6684–6689, Oct. 1998.
[6] M. Norgia, G. Giuliani, and S. Donati, "Absolute distance measurement with improved accuracy using laser diode self-mixing interferometry in a closed loop," *IEEE Trans. Instrum. Meas.*, vol. 56, no. 5, pp. 1894–1900, Oct. 2007.
[7] Y. Zhao, S. Wu, R. Xiang, and Z. Cao, "Self-mixing fiber ring laser velocimeter with orthogonal-beam incident system," *IEEE Photon. J.*, vol. 6, no. 2, p. 6801211, Apr. 2014.

[8] M. Norgia, A. Pesatori, and L. Rovati, "Self-mixing laser Doppler spectra of extracorporeal blood flow: A theoretical and experimental study," *IEEE Sensors J.*, vol. 12, no. 3, pp. 552–557, Mar. 2012.
[9] S. K. Özdemir, S. Takamiya, S. Ito, S. Shinohara, and H. Yoshida, "Self-mixing laser speckle velocimeter for blood flow measurement," *IEEE Trans. Instrum. Meas.*, vol. 49, no. 5, pp. 1029–1035, Oct. 2000.
[10] S. Donati, M. Norgia, and G. Giuliani, "Self-mixing differential vibrometer based on electronic channel subtraction," *Appl. Opt.*, vol. 45, no. 28, pp. 7264–7268, Oct. 2006.
[11] K. Otsuka, K. Abe, J.-Y. Ko, and T.-S. Lim, "Real-time nanometer-vibration measurement with a self-mixing microchip solid-state laser," *Opt. Lett.*, vol. 27, no. 15, pp. 1339–1341, Aug. 2002.
[12] Y. Huang, Z. Du, J. Deng, and X. Cai, "Study of vibration system characteristics based on laser self-mixing interference effect," *J. Appl. Phys.*, vol. 112, no. 2, pp. 023106–023106, Jul. 2012.
[13] Y. Yu, G. Giuliani, and S. Donati, "Measurement of the linewidth enhancement factor of semiconductor lasers based on the optical feedback self-mixing effect," *IEEE Photon. Technol. Lett.*, vol. 16, no. 4, pp. 990–992, Apr. 2004.
[14] R. Lang and K. Kobayashi, "External optical feedback effects on semiconductor injection laser properties," *IEEE J. Quantum Electron.*, vol. QE-16, no. 3, pp. 347–355, Mar. 1980.
[15] W. M. Wang, K. T. V. Grattan, A. W. Palmer, and W. J. O. Boyle, "Self-mixing interference inside a single mode diode laser for optical sensing applications," *J. Lightwave Technol.*, vol. 12, no. 9, pp. 1577–1587, Sep. 1994.
[16] G. Giuliani, M. Norgia, S. Donati, and T. Bosch, "Laser diode self-mixing technique for sensing applications," *J. Opt. A, Pure Appl. Opt.*, vol. 4, no. 6, pp. 283–294, 2002.
[17] L. Meirovitch, *Principles and Techniques of Vibrations*. Upper Saddle River, NJ, USA: Prentice-Hall, 1997.